Synthesis and Crystal Structure of a New Fluorogallophosphate Named Mu-12

A. Matijasic,[†] B. Marler,[‡] J. C. Muñoz Acevedo,[§] L. Josien,[†] and J. Patarin*[,†]

Laboratoire de Matériaux Minéraux, ENSCMu, Université de Haute-Alsace, UMR CNRS 7016, 3 rue Alfred Werner, 68093 Mulhouse Cedex, France, Institut für Mineralogie, Ruhr-Universität Bochum, D-44780 Bochum, Germany, and Facultad de Ciencias Físicas y Matematicas, Universidad de Chile, Blanco Encalada 2008, Laboratorio de Cristalografía, Santiago, Chile

Received November 28, 2002. Revised Manuscript Received March 30, 2003

In the present paper, the synthesis and structure determination of a new three-dimensional microporous fluorogallophosphate, named Mu-12, is reported. This material ($Ga_{20}P_{16}O_{72}F_4$-$[C_2N_2H_{10}]_4$) was obtained by hydrothermal synthesis in the presence of ethylenediamine as organic template, using the fluoride route. Its structure was determined by single-crystal X-ray diffraction. The symmetry is monoclinic, space group $P2_1/n$, with the following unit-cell parameters: $a = 14.3753(9)$ Å, $b = 11.9410(7)$ Å, $c = 10.1760(6)$ Å, and $\beta = 91.102(5)°$. The three-dimensional framework of Mu-12 can completely be built from ladder chains obtained by connection of four-membered rings (4MR), which consist of 2 Ga and 2 P atoms. These chains are connected to each other in the *a* and *b* directions through GaO_6 octahedra. The resulting three-dimensional framework displays a one-dimensional channel system parallel to the [100] direction delimited by 9-MR openings and hosting the protonated amine. This material was characterized by elemental and thermal analyses, XRD, SEM, and ^{13}C, ^{19}F, and ^{31}P solid-state NMR spectroscopy.

1. Introduction

Since the discovery of porous aluminophosphates by Wilson et al.,[1] a large number of phosphate-based materials has been prepared. It was the case in particular of gallophosphates. In these solids, gallium can adopt 4-, 5-, or 6-coordination and this particularity allows the building of a wide diversity of open-gallophosphate frameworks. Various synthesis routes have been used to prepare these materials. Besides the conventional route, which consists of a hydrothermal treatment of a gallophosphate mixture containing water and usually an organic structure-directing species, a large number of new solids were obtained from fluoride-containing mixtures.[2−4] Fluorine can be present in the as-synthesized material as terminal Ga−F groups, bridging gallium atoms or occluded in small structural units, the so-called double-four ring units. In the latter case, it would act in a structure-directing role by stabilizing these building units.[5] Among the various organic species used, the family of diaminoalkanes displays a strong templating effect.[6−9] In this family, ethylenediamine was used to prepare several gallophosphates using[10] or not using[11,12] the fluoride route. Recently, we reported the synthesis and the structure determination of a new ethylenediamine-containing hydroxyfluorogallophosphate named Mu-20.[13] It was obtained using 4,9-dimethyl-5,8-diaza-dodeca-2,4,8,10-tetraen-2,11-diol (hereafter called 3DTD) as organic species, the latter being decomposed in ethylenediamine during the hydrothermal treatment. In some cases, Mu-20 crystallized in the presence of an unknown phase (phase A in ref 13).

In the present paper, we report the synthesis and the single-crystal X-ray structure determination of this unknown phase. The latter was also obtained from either the decomposition of 3DTD or directly in the presence of ethylenediamine. This material, named in the present paper Mu-12, was characterized by several techniques such as XRD, chemical analysis, SEM, TG/DTA, and multinuclear solid-state NMR spectroscopy.

* To whom correspondence should be addressed. Tel.: 33 3 89 33 68 80. Fax: 33 3 89 33 68 85.
[†] Université de Haute-Alsace.
[‡] Ruhr-Universität Bochum.
[§] Universidad de Chile.

(1) Wilson, S. T.; Lok, B. M.; Messina, C. A.; Cannan, T. R.; Flanigen, E. M. *J. Am. Chem. Soc.* **1982**, *101*, 1146.
(2) Cheetham, A. K.; Férey, G.; Loiseau, T. *Angew. Chem., Int. Ed.* **1999**, *38*, 3268.
(3) Patarin, J.; Paillaud, J. L.; Kessler, H. *Handbook of Porous Solids*; Schüth, F., Sing, K. S. W., Weitkamp, J., Eds.; Wiley-VCH Verlag GmbH: Germany, 2002; Vol. 2, Chapter 4.2.3, p 815.
(4) Bonhomme, F.; Thoma, S. G.; Rodriguez, M. A.; Nenoff, T. M. *Chem. Mater.* **2001**, *13*, 2112.
(5) Matijasic, A.; Reinert, P.; Josien, L.; Simon, A.; Patarin, J. *Studies in Surface Science and Catalysis*; Galarneau, A., Di Renzo, F., Fajula, F., Vedrine, J., Eds.; Elsevier: Amsterdam, 2001; Vol. 135, p 142.
(6) Taulelle, F.; Samoson, A.; Loiseau, T.; Férey, G. *J. Phys. Chem. B* **1998**, *102*, 8588.
(7) Chippindale, A. M.; Walton, R. I.; Turner, C. *J. Chem. Soc., Chem. Commun.* **1995**, 1261.
(8) Reinert, P.; Marler, B.: Patarin, J. *Microporous Mesoporous Mater.* **2000**, *39*, 509.
(9) Matijasic, A.; Paillaud, J. L.; Patarin, J. *J. Mater. Chem.* **2000**, *10*, 1345.
(10) Loiseau, T. Ph.D. Thesis, University of Le Mans, Le Mans, 1994.
(11) Parise, J. B. *J. Chem. Soc., Chem. Commun.* **1985**, 606.
(12) Chippindale, A. M. *Chem. Mater.* **2000**, *12*, 818.
(13) Matijasic, A.; Gramlich, V.; Patarin, J. *J. Mater. Chem.* **2001**, *11*, 2553.

10.1021/cm021370k CCC: $25.00
Published on Web 06/05/2003

Table 1. Syntheses Performed at 170 °C in the System Ga_2O_3−P_2O_5−HF−S−H_2O (S for 4,9-Dimethyl-5,8-diaza-dodeca-2,4,8,10-tetraen-2,11-diol (3DTD) or Ethylenediamine (EDA))[a]

sample	organic species (S)	HF (x)	crystallization time (days)	XRD results
A	3DTD	0	4	$GaPO_4$−12
B	3DTD	0.5	4	Mu-12
C	3DTD	2	4	Mu-12 + Mu-20
D	EDA	0.25	4	Mu-12[b] + $GaPO_4$-12
E	EDA	0.5	4	Mu-12 + ULM-4
F	EDA	2	2	Mu-20

[a] Starting molar composition 1:1:x:0.5:80 Ga_2O_3:P_2O_5:HF:S:H_2O. The pH value was adjusted to 4−4.5 with tripropylamine (TRIPA); see text (0.8 TRIPA per 1 P_2O_5). [b] The underlined phase corresponds to the major phase.

2. Experimental Section

2.1. Reactants. As mentioned in ref 13, the 4,9-dimethyl-5,8-diaza-dodeca-2,4,8,10-tetraen-2,11-diol (3DTD) was prepared accidentally using a procedure described in the literature to synthesize the 5,7,12,14-tetramethyl-1,4,8,11-tetraazacyclotetradeca-4,7,11,14-tetraene.[14] Experiments were also performed in the presence of ethylenediamine (Aldrich, 98%) as structure-directing species. The other reactants were 85% aqueous phosphoric acid (H_3PO_4, Prolabo, Normapur) and 40% aqueous hydrofluoric acid (HF, Prolabo, Normapur). The gallium source was an amorphous gallium oxide hydroxide that was prepared by heating a gallium nitrate solution (Rhône-Poulenc) at 250 °C for 24 h.

2.2. Synthesis Procedure. Mu-12 was difficult to obtain as a pure phase. In most cases, it crystallized with other known materials such as $GaPO_4$-12,[11] ULM-4,[15] and Mu-20[13] (see Table 1). The best sample was prepared after hydrothermal treatment of a mixture having the following molar composition: 1:1:0.5:0.5:80 Ga_2O_3:P_2O_5:HF:3DTD:H_2O.

As an example, for sample B (Table 1), the gel was prepared by adding, under stirring, the gallium source (0.90 g) to H_3PO_4 (0.92 g) and water (5.6 g). After homogenization, HF (0.10 g) and 3DTD (0.45 g) were successively introduced. The pH value was adjusted to 4−4.5 with tripropylamine, the latter presenting no structure-directing effect in the fluorine-containing gallophosphate system.[16] The resulting gel was mixed at room temperature for 1 h and transferred into a 20-mL PTFE-lined stainless steel autoclave. The crystallization was carried out at 170 °C under static conditions. After 4 days of heating, the product was recovered, washed with distilled water, and dried at 60 °C overnight.

2.3. Thermal Analysis. Prior to analysis, the solids were kept in a wet atmosphere over a saturated aqueous solution of NH_4Cl (P/P_0 = 0.85) for 24 h to set the hydration state. Thermogravimetric (TGA) and differential thermal (DTA) analyses were performed under air on a Setaram Labsys thermoanalyzer with a heating rate of 5 °C/min.

2.4. Powder X-ray Diffraction. The XRD powder data were recorded, in Debye−Scherrer geometry, on a STOE STADI-P diffractometer, equipped with a curved germanium (111) primary monochromator and a linear position-sensitive detector (6° 2θ) using Cu Kα_1 radiation (λ = 1.5406 Å). The simulated XRD pattern was calculated from the structure data using the STOE Win XPOW software. A Huber photographic chamber (model 631) was used for the high-temperature XRD analysis, the latter also being performed using Cu Kα_1 radiation.

2.5. Chemical Analysis. Ga and P analysis was performed by inductively coupled plasma emission spectroscopy. F^- content was determined using a fluoride ion-selective electrode after mineralization and C and N analyses by coulometric and catharometric determinations, respectively, after calcination of the samples.

The Ga, P, O, and F contents were also determined by microprobe analysis on a Castaing-type (Camebax) scanning electron microscope.

Table 2. Recording Conditions of the MAS and CP MAS NMR Spectra

	^{19}F	^{13}C	^{31}P	
	MAS	CP MAS	MAS	CP MAS
chemical shift standard	$CFCl_3$	TMS	85% H_3PO_4	
frequency (MHz)	376.5	75.47	161.98	
pulse width (μs)	3	6.5	3	
flip angle	π/2	π/2	π/2	
contact time (ms)	/	2	/	0.1
recycle time (s)	20	4	8	
spinning rate (Hz)	10000	5000	8000	
number of scans	24	1450	56	

2.6. ^{13}C, ^{19}F, and ^{31}P Solid-State NMR Spectroscopy. The ^{13}C CP MAS NMR spectrum was recorded on a Bruker MSL 300 spectrometer and ^{19}F and ^{31}P NMR spectra on a Bruker DSX 400 spectrometer. The recording conditions of the CP MAS and MAS spectra are given in Table 2.

2.7. Structure Determination. For the structure determination, a single crystal with dimensions of ca. 80 × 100 × 140 μm^3 was selected from the batch and mounted on a Xcalibur automated four-circle diffractometer, with Kappa configuration. 6607 reflections were recorded up to 68.24° 2θ (using Mo Kα radiation) in ω scan mode. A summary of the experimental and crystallographic data is reported in Table 3.

Special care was taken to use a nontwinned crystal for the structure analysis: Optical examination of the analyzed crystal using a polarization microscope showed sharp extinction between crossed nicols. During the single-crystal data collection (CCD detector) there was no indication of a second set of reflections which could not be indexed by the given orientation matrix. The simulated powder pattern being calculated from the structure data as obtained by the single-crystal structure refinement is nearly identical to the experimental pattern of the Mu12 material (see Figure 2). We therefore concluded that the analyzed crystal was not twinned.

The structure was solved by direct methods using SHELXS97[17] and refined using SHELXL97.[18] The refinement converged to R1 = 0.0446 (R1 = $\Sigma||F_o| - |F_c||/\Sigma|F_o|$) for 3752 reflections ($I > 4\sigma(I)$) and R1 = 0.1014 and wR2 = 0.1692 (R2 = $\{\Sigma w(F_o^2 - F_c^2)^2/\Sigma w(F_o^2)^2\}^{1/2}$) for all data. The positions of the hydrogen atoms of the organic species could not be determined. Indeed, the carbon and nitrogen atoms of the organic species show considerable positional disorder; therefore, it was not meaningful to calculate the possible positions of the hydrogen atoms based on geometric constraints. All atoms were refined with anisotropic displacement parameters except one highly disordered nitrogen atom, which was refined using split positions with isotropic displacement parameters. The occupancy factors (PP) of F1 and F2 as well as those of N21, N22, and N23 were refined such that $PP_{F(1)} + PP_{F(2)} = 1$ and $PP_{N(21)} + PP_{N(22)} + PP_{N(23)} = 1$. The atomic coordinates and isotropic displacement parameters are given in Table 4; selected bond lengths and angles are reported in Tables 5 and 6, respectively.

3. Results and Discussion

3.1. Synthesis and Crystal Morphology. In Table 1 are summarized the most characteristic synthesis

(14) Singh, A. K.; Chandra, S.; Baniwal, S. *J. Indian. Chem. Soc.* **1998**, *75*, 84.
(15) Cavellec, M.; Riou, D.; Férey, G. *Eur. J. Solid State Inorg. Chem.* **1994**, *31*, 583.
(16) Schott-Darie, C. Ph.D. Thesis, University of Haute Alsace, Mulhouse, 1994.
(17) Sheldrick, G. M. *Programs for the crystal structure analysis SHELXS97* (Release 97-2); Department of Anorganic Chemistry, University of Göttingen: Göttingen, Germany, 1998.
(18) Sheldrick, G. M. *Programs for the crystal structure analysis SHELXL97* (Release 97-2); Department of Anorganic Chemistry, University of Göttingen: Göttingen, Germany, 1998.

Table 3. Experimental and Crystallographic Parameters for the Structure Analysis of the Fluorogallophosphate Mu-12

chemical formula	$Ga_5P_4O_{18}F[C_2N_2H_{10}]$
crystal system	monoclinic
crystal space group	$P2_1/n$
a (Å)	14.3753(9)
b (Å)	11.9410(7)
c (Å)	10.1760(6)
β (deg)	91.102(5)
formula weight ($g \cdot mol^{-1}$)	831.5
density (calcd) ($g \cdot mL^{-1}$)	3.162
cell volume (Å^3)	1746.44
Z (formula units/cell)	4
crystal size (μm^3)	ca. 80 × 100 × 140
diffractometer	Xcalibur automated four-circle diffractometer with Kappa configuration, and CCD detector
radiation source and wavelength (Å)	Mo Kα, 0.7107
absorption coefficient (mm^{-1})	8.09
absorption correction	numerical
data collection temperature (K)	293
θ range (deg)	0−68.24
(hkl)min., (hkl)max.	$-22 \le h \le 21$, $-18 \le k \le 17$, $-15 \le l \le 16$
independent reflns	6607
observed reflns	3752
observation criterion	$I > 4\sigma(I)$
data/restraints/ parameters	3752/1/303
structure solution program	SHELXS97
structure refinement program	SHELXL97
residuals (observed data)	R1 = 0.0446 ($R1 = \Sigma\|\|F_o\| - \|F_c\|\|/\Sigma\|F_o\|$)
residuals (all data)	R1= 0.1014 wR2 = 0.1692 ($wR2 = \{\Sigma w(F_o^2 - F_c^2)^2/\Sigma w(F_o^2)^2\}^{1/2}$)
goodness-of-fit (all data)	0.974
largest diff. peak and hole (e/Å^3)	maximum = +1.71, minimum = −1.01

Table 4. Atomic Coordinates (Å × 10^4), Equivalent Isotropic Displacement Parameters (Å^2 × 10^3), and the Occupancy Factors (PP) for the Fluorogallophosphate Mu-12; Standard Deviations in Parentheses[a]

atoms	x	y	z	U(eq)	PP
Ga(1)	2489(1)	5007(1)	4965(1)	9(1)	1
Ga(2)	876(1)	3750(1)	6734(1)	14(1)	1
Ga(3)	4110(1)	3618(1)	3457(1)	13(1)	1
Ga(4)	−863(1)	3678(1)	3398(1)	12(1)	1
Ga(5)	4094(1)	6337(1)	3308(1)	12(1)	1
P(1)	1252(1)	3008(1)	3921(1)	11(1)	1
P(2)	−1235(1)	3072(1)	6245(1)	10(1)	1
P(3)	3758(1)	6977(1)	6112(1)	10(1)	1
P(4)	6235(1)	6882(1)	3707(1)	12(1)	1
O(1)	1310(2)	5005(2)	5928(3)	14(1)	1
O(2)	3676(2)	4991(2)	3913(3)	13(1)	1
O(3)	2094(2)	3767(3)	3826(3)	16(1)	1
O(4)	2928(2)	6195(3)	6157(3)	13(1)	1
O(5)	410(2)	3590(3)	3250(3)	14(1)	1
O(6)	−2069(2)	3853(3)	6295(3)	14(1)	1
O(7)	−403(2)	3659(3)	6916(3)	17(1)	1
O(8)	1436(2)	1890(3)	3196(3)	16(1)	1
O(9)	4610(2)	6388(3)	6730(3)	17(1)	1
O(10)	−1443(2)	1999(3)	7015(3)	18(1)	1
O(11)	−1021(2)	2709(3)	4837(3)	15(1)	1
O(12)	7034(2)	6058(3)	3707(3)	18(1)	1
O(13)	6050(2)	7301(3)	5110(3)	17(1)	1
O(14)	5362(2)	6315(3)	3083(3)	17(1)	1
O(15)	3558(2)	8038(3)	6876(3)	18(1)	1
O(16)	6486(2)	7915(3)	2901(3)	21(1)	1
O(17)	1076(2)	2694(3)	5365(3)	15(1)	1
O(18)	3949(2)	7347(3)	4685(3)	15(1)	1
F(1)	681(3)	5089(3)	8140(3)	20(1)	0.778(6)[a]
F(2)	4360(10)	4930(10)	1830(10)	22(3)	0.222(6)[a]
C(1)	2236(7)	9757(8)	5270(10)	77(3)	1
C(2)	2851(7)	10140(10)	4250(10)	109(5)	1
N(1)	3793(6)	9812(6)	4198(8)	80(2)	1
N(21)	1230(20)	10150(20)	5730(30)	47(2)	0.27(1)
N(22)	1620(20)	10480(20)	6160(20)	47(2)	0.29(2)
N(23)	2160(10)	10550(10)	6200(10)	47(2)	0.44(2)

[a] U(eq) is defined as one-third the trace of the $\mathbf{U}_{ij}$ tensor. To obtain more realistic occupancy factors for the split positions of N(2) (N(21), N(22), N(23)), the isotropic displacement parameters were constraint to be equal. The occupancy factors of F(1) and F(2) as well as those of N(21), N(22), and N(23) were refined such that $PP_{F(1)} + PP_{F(2)} = 1$ and $PP_{N(21)} + PP_{N(22)} + PP_{N(23)} = 1$.

results obtained using 3DTD or ethylenediamine (EDA) as organic template. It is worthy to note that, under the synthesis conditions used, 3DTD decomposes into EDA. This was clearly evidenced by ^{1}H and ^{13}C liquid NMR spectroscopy.[13] Therefore, in all cases the structure-directing agent is ethylenediamine. However, for the 3DTD-containing mixtures, the in situ formation of EDA seems to be responsible of the formation of new phases as it was previously observed for the synthesis in the presence of alkylformamides of the aluminophosphates Mu-4 and Mu-7.[19,20] In the absence of fluoride anions (x = 0 HF, sample A), the gallophosphate $GaPO_4$-12, which is well-known to be formed from an ethylenediamine-containing gallophosphate gel, crystallizes. Synthesis performed in the presence of 3DTD with large amounts of fluoride (x = 2 HF, sample C) leads to the formation of a mixture of Mu-12 and the hydroxyfluorogallophosphate Mu-20. Under similar synthesis conditions, but with a shorter crystallization time, the latter material is obtained as pure phase in the presence of EDA (sample F). On the other hand, the introduction of a small amount of fluoride in a 3DTD-containing mixture allows the preparation of a pure Mu-12 phase (sample B), whereas when ethylenediamine is introduced in the starting gel, the product consists of a mixture of Mu-12 and the fluorogallophosphate ULM-4 (sample E).

SEM micrographs of the fluorogallophosphate Mu-12 (sample B) are shown in Figure 1. The material displays a spherelike morphology. Large spherical aggregates with a size close to 50 μm consisting of prismatic crystals are present. The crystal size is ranging from 10 to 20 × 5−10 × 5−10 μm^3. For the structure determination a large single crystal was selected from batch D (mixture of Mu-12 and $GaPO_4$-12).

A typical powder XRD pattern of the fluorogallophosphate Mu-12 (sample B) is given in Figure 2a. This pattern can be indexed in the monoclinic symmetry with the following unit cell parameters: a = 14.342(3) Å, b = 11.932(2) Å, c = 10.164(2) Å, and β = 91.11(2)°. For comparison, the simulated XRD pattern calculated from the structure data is also reported (Figure 2b).

3.2. Chemical Analyses. According to the chemical, microprobe, and thermal analyses, the as-synthesized Mu-12 sample (sample B) has the following composition

(19) Vidal, L.; Gramlich, V.; Patarin, J.; Gabelica, Z. *Eur. J. Solid State Inorg. Chem.* **1998**, *35*, 545.
(20) Vidal, L.; Marichal, C.; Gramlich, V.; Patarin, J.; Gabelica, Z. *Chem. Mater.* **1999**, *11*, 2728.

Table 5. Selected Bond Lengths of the Structure of Mu-12; Standard Deviations Are Given in Parentheses[a]

atoms	distances (Å)	atoms	distances (Å)	atoms	distances (Å)
Ga(1)−O(6)#3	1.958(3)	Ga(4)−O(16)#2	1.826(3)	P(3)−O(15)	1.517(3)
Ga(1)−O(4)	1.962(3)	Ga(4)−O(5)	1.842(3)	P(3)−O(9)	1.536(3)
Ga(1)−O(1)	1.974(3)	Ga(4)−O(1)#3	1.835(3)	P(3)−O(4)	1.517(3)
Ga(1)−O(3)	1.958(3)	Ga(4)−O(11)	1.884(3)	P(3)−O(18)	1.547(3)
Ga(1)−O(12)#3	1.969(3)	**⟨Ga(4)−O⟩**	**1.847**	**⟨O−P(3)−O⟩**	**1.529**
Ga(1)−O(2)	2.032(3)	Ga(4)−F(1)#3	2.169(4)		
⟨O−Ga(1)−O⟩	**1.992**	**⟨Ga(4)−O/F⟩**	**1.911**	P(4)−O(16)	1.529(3)
				P(4)−O(14)	1.551(3)
Ga(2)−O(1)	1.825(3)	Ga(5)−O(8)#2	1.821(3)	P(4)−O(13)	1.540(3)
Ga(2)−O(7)	1.853(3)	Ga(5)−O(14)	1.842(3)	P(4)−O(12)	1.512(3)
Ga(2)−O(15)#2	1.828(3)	Ga(5)−O(2)	1.827(3)	**⟨O−P(4)−O⟩**	**1.533**
Ga(2)−O(17)	1.905(3)	Ga(5)−O(18)	1.864(3)		
⟨Ga(2)−O⟩	**1.853**	**⟨Ga(5)−O⟩**	**1.838**	C(1)−C(2)	1.45(2)
Ga(2)−F(1)	2.167(3)	Ga(5)−F(2)	2.29(1)	C(1)−N(21)	1.60(3)
⟨Ga(2)−O/F⟩	**1.916**	**⟨Ga(5)−O/F⟩**	**1.929**	C(2)−N(1)	1.41(1)
				C(1)−N(22)	1.54(3)
Ga(3)−O(2)	1.817(3)	P(1)−O(3)	1.517(3)	C(1)−N(23)	1.35(2)
Ga(3)−O(9)#3	1.853(3)	P(1)−O(5)	1.542(3)		
Ga(3)−O(10)#4	1.812(3)	P(1)−O(17)	1.542(3)	N(1)−F(1)#2	2.82(1)
⟨Ga(3)−O⟩	**1.831**	P(1)−O(8)	1.550(3)	N(22)−O(17)#1	2.87(2)
Ga(3)−F(2)	2.32(1)	**⟨O−P(1)−O⟩**	**1.538**	N(23)−O(4)#2	2.80(1)
⟨Ga(3)−O/F⟩	**1.928**			N(21)−F(2)#2	2.73(3)
		P(2)−O(6)	1.520(3)	N(22)−O(4)#2	2.93(2)
		P(2)−O(10)	1.534(3)	N(23)−O(16)#3	2.81(2)
		P(2)−O(11)	1.533(3)		
		P(2)−O(7)	1.536(3)		
		⟨O−P(2)−O⟩	**1.531**		

[a] Symmetry operations used to generate equivalent atoms: #1: x, y, z; #2: $-x + 1/2, y + 1/2, -z + 1/2$; #3: $-x, -y, -z$; #4: $x - 1/2, -y - 1/2, z - 1/2$.

(wt %): Ga, 40.1; P, 14.3; F, 2.2; N, 3.4; C, 2.9. The C/N molar ratio is close to 1. It corresponds to that of the ethylenediamine molecule and clearly shows that the latter (∼7.0 wt %) is occluded in the structure. The Ga/P molar ratio (1.25) is quite different from the one usually observed in the GaPO system, that is, 1.[3]

The whole of these analyses is in good agreement with the unit cell formula found by the structure analysis: $Ga_{20}P_{16}O_{72}F_4[C_2N_2H_{10}]_4$. In this formula, the amine is supposed to be doubly protonated.

3.3. Thermal Analyses. The thermal stability under air of Mu-12 was investigated using high-temperature XRD analysis and TG/DTA thermal analysis. The TG and DTA curves of the as-synthesized Mu-12 sample are given in Figure 3. The total weight loss, close to 9.6%, corresponds to the removal of the organic species and the removal of HF and occurs mainly in two steps. The first one (about 7.0 wt %), before 550 °C, leads to an endothermic peak followed by an exothermic one on the DTA curve and can be assigned to the decomposition of ethylenediamine, whereas the second one between 550 and 700 °C (2.6 wt %) seems to be associated with no visible thermal effect and could correspond to the departure of fluorine. According to the high-temperature XRD analysis, the structure is stable until 550 °C but slight variations can be observed on the XRD pattern. After the second weight loss, the structure collapses and a recrystallization into dense phases ($GaPO_4$-quartz or tridymite) occurs.

3.4. Description of the Structure. *The Framework.* The 3-D open framework structure of Mu-12 consists of a network of GaO_6, GaO_4, GaO_4F, and PO_4 polyhedra. There are five and four distinct crystallographic sites for gallium and phosphorus atoms, respectively. From the careful chemical and microprobe analyses only one F atom is present per formula unit ($Ga_5P_4O_{18}F$-$[C_2N_2H_{10}]$). However, according to the structure refinement, this fluorine atom is distributed over two different positions (F(1) and F(2), see Table 4) with occupation factors of 0.778(6) and 0.222(6), respectively.

For a first attempt only one fluorine position had been included in the structure analysis. The examination of the list of remaining difference electron maxima, however, showed one prominent maximum with an electronic density of 3.76 e/Å^3 (deepest hole = −1.02 e/Å^3, mean = 0.01 e/Å^3). Moreover, the refinement of the occupancy factor of F(1) (at that stage of refinement) led to a value of 0.62(1). The electron density maximum showed distances of 2.26 Å to Ga(5), 2.38 Å to Ga(3), 2.38 Å to O(2), and 2.50 Å to O(14) as the nearest neighbors and was therefore regarded to represent another position of the fluorine atom.

Since the chemical and microprobe analyses gave exactly one fluorine atom per formula unit and since charge balance between framework and $[C_2N_2H_{10}]^{2+}$ guest ion requires one negative charge in addition to the $[Ga_5P_4O_{18}]^-$ unit, the occupancy factors (PP) of F(1) and F(2) were constrained to $PP_{F(1)} + PP_{F(2)} = 1$ in the final refinement cycles. The distribution of the fluorine atom between two split positions has consequences for the arrangement of the guest ion (see below).

As was previously observed in the hexameric $Ga_3(PO_4)_3F_2$ and pentameric $Ga_3(PO_4)_2F_4$ units of several fluorogallophosphates,[21,22] F atom, in both positions, bridges two gallium atoms, increasing the coordination number from 4 to 5. The statistical distribution of the fluorine atoms about two sites (F(1) with an occupancy factor of 0.78 and F(2) with an occupancy factor of 0.22) gives rise to several different geometric arrangements: The asymmetric unit can contain 2 fluorine atoms on

(21) Loiseau, T.; Férey, G. *J. Solid State Chem.* **1994**, *111*, 403.
(22) Sassoye, C.; Marrot, J.; Loiseau, T.; Férey, G. *Chem. Mater.* **2002**, *14*, 1340.

Table 6. Selected Angles of the Structure of Mu-12; Standard Deviations Are Given in Parentheses[a]

atoms	angles (deg)	atoms	angles (deg)
O(6)−Ga(1)#3−O(3)	93.2(1)	O(1)−Ga(2)−O(7)	116.2(1)
O(3)−Ga(1)−O(12)#3	90.6(2)	O(1)−Ga(2)−O(17)	99.0(1)
O(6)−Ga(1)#3−O(1)	94.0(1)	O(7)−Ga(2)−O(17)	101.4(1)
O(4)−Ga(1)−O(1)	87.9(1)	O(15)−Ga(2)#2−O(7)	108.8(1)
O(6)−Ga(1)#3−O(2)	84.9(1)	O(15)−Ga(2)#2−O(17)	100.8(1)
O(4)−Ga(1)−O(2)	93.9(1)	O(1)−Ga(2)−O(15)#2	125.4(1)
O(6)−Ga(1)#3−O(4)	89.6(2)	⟨**O−Ga(2)−O**⟩	**108.6**
O(4)−Ga(1)−O(12)#3	86.6(1)	O(15)−Ga(2)#2−F(1)	83.9(1)
O(3)−Ga(1)−O(1)	92.8(1)	O(17)−Ga(2)−F(1)	173.9(1)
O(12)−Ga(1)#3−O(1)	87.1(1)	O(7)−Ga(2)−F(1)	80.6(1)
O(3)−Ga(1)−O(2)	85.3(1)	O(1)−Ga(2)−F(1)	74.9(1)
O(12)−Ga(1)#3−O(2)	94.1(1)		
⟨**O−Ga(1)−O**⟩	**90.0**	O(16)−Ga(4)#2−O(1)#3	121.8(1)
O(6)−Ga(1)#3−O(12)#3	176.0(1)	O(16)−Ga(4)#2−O(5)	112.8(1)
O(3)−Ga(1)−O(4)	177.0(1)	O(16)−Ga(4)#2−O(11)	101.0(2)
O(1)−Ga(1)−O(2)	177.8(1)	O(5)−Ga(4)−O(11)	99.4(1)
⟨**O−Ga(1)−O**⟩	**176.9**	O(1)−Ga(4)#3−O(5)	115.7(1)
		O(1)−Ga(4)#3−O(11)	100.8(1)
O(10)−Ga(3)#4−O(13)#3	109.8(2)	⟨**O−Ga(4)−O**⟩	**108.6**
O(10)−Ga(3)#4−O(9)#3	109.7(2)	O(1)−Ga(4)#3−F(1)#3	74.7(1)
O(13)−Ga(3)#3−O(9)#3	102.7(1)	O(11)−Ga(4)−F(1)#3	175.1(1)
O(2)−Ga(3)−O(13)#3	106.6(1)	O(5)−Ga(4)−F(1)#3	81.1(1)
O(2)−Ga(3)−O(9)#3	112.0(1)	O(16)−Ga(4)#2−F(1)#3	83.1(1)
O(10)−Ga(3)#4−O(2)	115.2(1)		
⟨**O−Ga(3)−O**⟩	**109.3**	O(8)−Ga(5)#2−O(14)	107.4(1)
O(2)−Ga(3)−F(2)	68.3(3)	O(8)−Ga(5)#2−O(18)	110.3(1)
O(9)−Ga(3)#3−F(2)	76.3(3)	O(14)−Ga(5)−O(18)	103.2(1)
O(13)−Ga(3)#3−F(2)	173.5(3)	O(2)−Ga(5)−O(14)	111.3(1)
O(10)−Ga(3)#4−F(2)	76.4(3)	O(2)−Ga(5)−O(18)	105.8(1)
		O(8)−Ga(5)#2−O(2)	117.9(1)
		⟨**O−Ga(5)−O**⟩	**109.3**
		O(2)−Ga(5)−F(2)	68.7(3)
		O(18)−Ga(5)−F(2)	172.1(3)
		O(14)−Ga(5)−F(2)	74.5(3)
		O(8)−Ga(5)#2−F(2)	77.6(3)
O(3)−P(1)−O(5)	108.8(2)	O(15)−P(3)−O(9)	109.3(2)
O(3)−P(1)−O(8)	109.9(2)	O(15)−P(3)−O(18)	106.3(2)
O(5)−P(1)−O(8)	108.4(2)	O(9)−P(3)−O(18)	111.2(2)
O(17)−P(1)−O(5)	113.0(2)	O(4)−P(3)−O(9)	109.1(2)
O(17)−P(1)−O(8)	106.0(2)	O(4)−P(3)−O(18)	111.0(2)
O(3)−P(1)−O(17)	110.6(2)	O(15)−P(3)−O(4)	110.0(2)
⟨**O−P(1)−O**⟩	**109.5**	⟨**O−P(3)−O**⟩	**109.5**
O(6)−P(2)−O(10)	109.5(2)	O(12)−P(4)−O(13)	110.8(2)
O(6)−P(2)−O(7)	108.3(2)	O(12)−P(4)−O(14)	108.9(2)
O(10)−P(2)−O(7)	108.2(2)	O(13)−P(4)−O(14)	111.7(2)
O(11)−P(2)−O(10)	106.6(2)	O(16)−P(4)−O(13)	106.4(2)
O(11)−P(2)−O(7)	112.0(2)	O(16)−P(4)−O(14)	109.3(2)
O(6)−P(2)−O(11)	112.1(2)	O(12)−P(4)−O(16)	109.8(2)
⟨**O−P(2)−O**⟩	**109.5**	⟨**O−P(4)−O**⟩	**109.5**
Ga(2)−O(1)−Ga(1)	121.9(2)	Ga(2)−O(1)−Ga(4)#3	114.2(2)
Ga(4)−O(1)#3−Ga(1)	119.6(2)	Ga(5)−O(2)−Ga(1)	117.1(2)
Ga(3)−O(2)−Ga(5)	126.2(2)	Ga(3)−O(2)−Ga(1)	116.0(2)
P(1)−O(3)−Ga(1)	129.6(2)	P(3)−O(4)−Ga(1)	132.1(2)
P(1)−O(5)−Ga(4)	139.5(2)	P(2)−O(6)−Ga(1)#3	129.6(2)
P(2)−O(7)−Ga(2)	138.4(2)	P(1)−O(8)−Ga(5)#2	129.8(2)
P(3)−O(9)−Ga(3)#3	138.1(2)	P(2)−O(10)−Ga(3)#4	131.8(2)
P(2)−O(11)−Ga(4)	125.6(2)	P(4)−O(12)−Ga(1)#3	132.4(2)
P(4)−O(13)−Ga(3)#3	124.5(2)	P(4)−O(14)−Ga(5)	137.5(2)
P(3)−O(15)−Ga(2)#2	134.3(2)	P(4)−O(16)−Ga(4)#2	132.3(2)
P(1)−O(17)−Ga(2)	124.4(2)	P(3)−O(18)−Ga(5)	123.0(2)

[a] Symmetry operations used to generate equivalent atoms: #1: x, y, z; #2: $-x + {}^1/_2, y + {}^1/_2, -z + {}^1/_2$; #3: $-x, -y, -z$; #4: $x - {}^1/_2, -y - {}^1/_2, z - {}^1/_2$.

the F(1) and F(2) positions, 1 fluorine atom on the F(1) or F(2) position, or no fluorine atoms. The structure will be described assuming that only two types of asymmetric units are present which contain fluorine either on the F(1) or on the F(2) position. Thus, in 78% of the asymmetric units, the fluorine F(1) bridges Ga(2) and Ga(4) by generating two GaO_4F polyhedra while the Ga(3) and Ga(5) atoms correspond to GaO_4 polyhedra (see Figure 4a). In 22% of the asymmetric units fluorine bridges F(2) are located between Ga(3) and Ga(5) and form GaO_4F polyhedra while the Ga(2) and Ga(4) atoms correspond to GaO_4 polyhedra (see Figure 4b). The connectivity scheme of the gallium polyhedra leads to the formation of a pentameric unit $Ga_5(PO_4)_4F$ (on the basis of the number of gallium polyhedra), which can be considered as the fundamental building block (Figure 4a,b). In this unit, a gallium octahedron (GaO_6) shares two of its oxygens (O(1) and O(2) atoms) with two GaO_4F polyhedra and two GaO_4 polyhedra and its other oxygen vertexes with four PO_4 tetrahedra. Oxygen atoms O(1) and O(2) thus bridge three metal centers. Such a situation is observed in some phosphate-based materials. It is the case for instance for the iron phosphate leucophosphite,[23,24] the aluminophosphate UIO-26,[25] the gallophosphate $GaPO_4$-12,[26] the large pore open framework gallium phosphate $[NH_3(CH_2)_4NH_3]_2[Ga_4(HPO4)_2(PO_4)_3(OH)_3]\cdot yH_2O$,[27] or the hydroxyfluorogallophosphate Mu-8[8] where oxo- or hydroxo groups are connected to three metal atoms.

The question whether O(1) and O(2) connect GaO_4F polyhedra or GaO_4 polyhedra to the central GaO_6 octahedron depends on which of the two fluorine positions is occupied (see Figure 4a,b).

The structure can be described as ladder chains built from single four rings $[Ga_2P_2]$ running along the *c* direction (Figure 5a,b). These chains are connected to each other in the *b* and *a* directions through the GaO_6 octahedra (Figure 5c,d, respectively). The resulting three-dimensional framework displays a one-dimensional channel system parallel to the [100] direction delimited by 9-MR openings (Figure 6) and hosting the protonated amine. Such pore openings are quite unusual. To our knowledge, among the 136 different zeolite structure types[28] only six 9-ring structures were reported. It was the case of the beryllosilicates chavennite (−CHI structure type) and lovdarite (LOV structure type), the zincosilicates RUB-17 and VPI-7 ((RSN and VSV structure types, respectively), the aluminosilicate natrolite (NAT structure type), and the silicate SSZ-23 (STT structure type).

In Mu-12, the $Ga(1)O_6$ octahedron is only slightly distorted, possessing Ga−O distances in the range of 1.958−2.032 Å with a mean value of 1.976 Å. The average angles in the GaO_6 octahedron are 176.9° and 90.0°. These values are quite typical for gallophosphates. Ga(2), Ga(3), Ga(4), and Ga(5) are part of more or less distorted GaO_4 tetrahedra if the fluorine atom is ignored as a ligand. The distortion is significant for $Ga(2)O_4$ and $Ga(4)O_4$ since Ga(2) and Ga(4) are interconnected by F(1) bridges (occupied to 78%) of medium length (Ga(2)−F(1) = 2.17 Å, Ga(4)−F(2) = 2.17 Å). For example, the Ga(2)−O distances are in the range of 1.825−1.905 Å and the O−Ga(2)−O angles vary between 99.0 and 125.4°. The average Ga−O distances are 1.853 and 1.847 Å for Ga(2) and Ga(4), respectively.

Because of the relatively large Ga(3)−F(2) and Ga(5)−F(2) distances and because of the low occupancy of

(23) Dick, S.; Zeiske, T. *J. Solid State Chem.* **1997**, *133*, 508.
(24) Moore, P. B. *Am. Mineral.* **1972**, *57*, 397.
(25) Konshaug, K. O.; Fjellvag, H.; Lillerud, K. P. *Microporous Mesoporous Mater.* **2000**, *40*, 313.
(26) Parise, J. B. *Inorg. Chem.* **1985**, *24*, 4312.
(27) Chippindale, A. M.; Peacock, K. J.; Cowley, A. R. *J. Solid State Chem.* **1999**, *145*, 379.
(28) Baerlocher, C.; Meier, W. M.; Olson, D. H. *Atlas of Zeolite Framework Types*, fifth edition; Elsevier: Amsterdam, 2001; p 302.

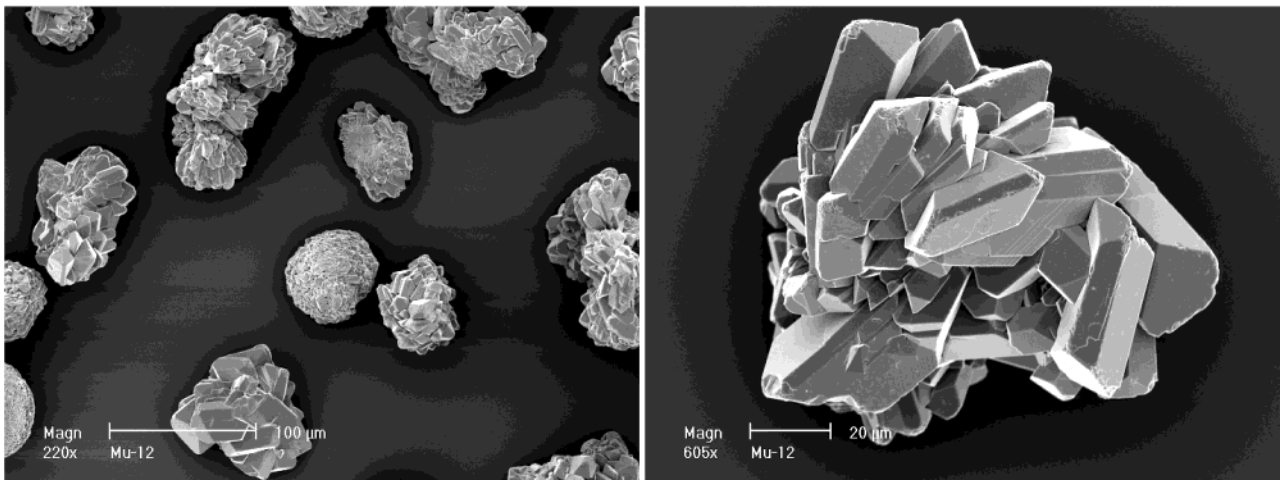

Figure 1. Scanning electron micrographs of the fluorogallophosphate Mu-12.

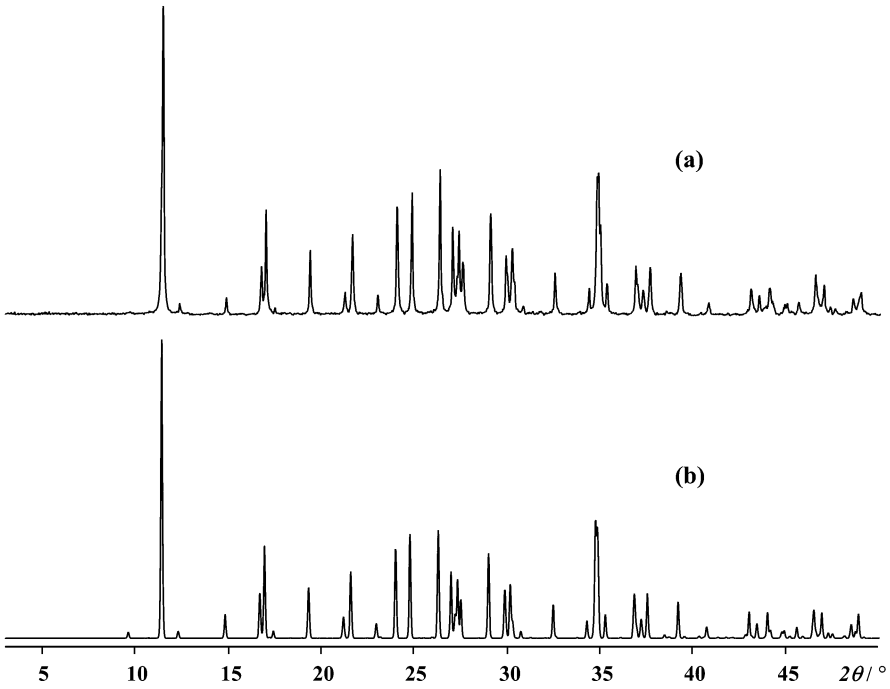

Figure 2. Powder XRD patterns of the fluorogallophosphate Mu-12: (a) experimental; (b) simulated from the structure data (radiation Cu $K\alpha_1$).

the F(2) position (22%), the $Ga(3)O_4$ and $Ga(5)O_4$ polyhedra are only very slightly distorted: for example, the Ga(3)−O distances are in the range of 1.812−1.853 Å and the O−Ga(3)−O angles vary between 102.7 and 115.2°. The average Ga−O distances for Ga(3) and Ga(5) are 1.831 and 1.838 Å, respectively. For details see Table 5.

Including the fluorine atoms average Ga−(O,F) distances of the GaO_4F polyhedra are 1.916, 1.928, 1.911, and 1.929 Å for Ga(2), Ga(3), Ga(4), and Ga(5), respectively. These are rather large values for GaO_4F polyhedra and can be explained by the fact that the fluorine atoms have relatively large distances to the Ga atoms.

Similar to the values usually observed for gallophosphates, the PO_4 tetrahedra of the title compound are quite regular polyhedra with P−O distances between 1.512 and 1.551 Å and tetrahedral angles O−P−O ranging from 106.0 to 113.0°.

The Guest Ions. The ethylenediamine molecules acting as templates for the formation of the title compound are occluded in the structure as double-protonated diammonium ions. The refined carbon and nitrogen positions do not represent the exact geometry of the occluded template since C−C and C−N distances differ somewhat from the expected values of 1.47 and 1.54 Å, respectively (see Table 5). This is interpreted to be due to positional disorder of the guest ion. Figure 7 shows the positions of the carbon and nitrogen atoms in the 9-MR channel as obtained from the refinement. The positional disorder of the ethylenediammonium ion in the title compound is mainly due to the fact that the F(1) and F(2) positions are statistically occupied by fluorine atoms. This leads to slightly different positions of the ethylenediammonium ion, which is bonded to the framework via F or O atoms depending on whether the F(1) or the F(2) site is occupied.

The main positional variation is observed for the $-N(2)H_3$ group. If only one position was refined for the N(2) atom, an extremely high displacement parameter resulted for this atom (U11 = 0.410 $Å^2$), reflecting a

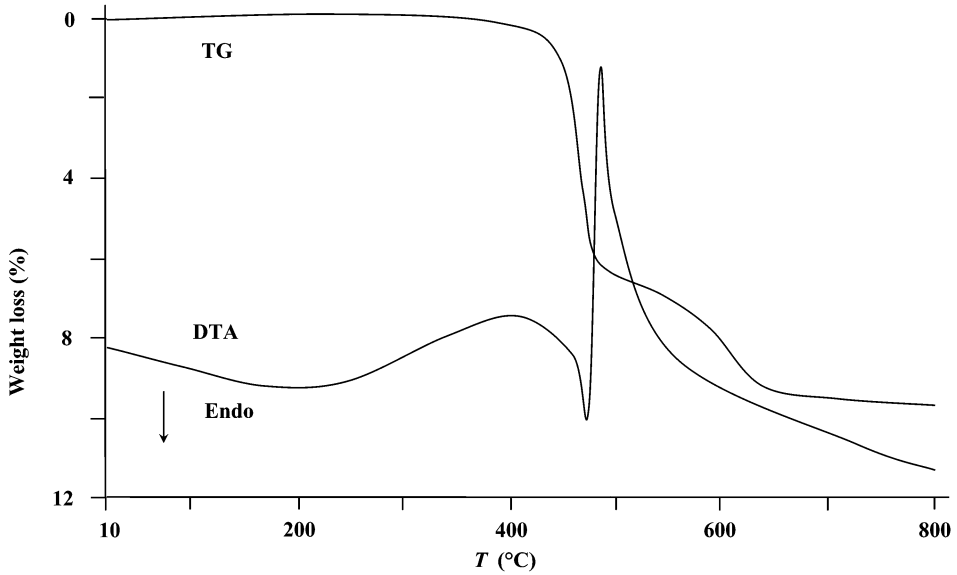

Figure 3. Thermal analysis of the fluorogallophosphate Mu-12.

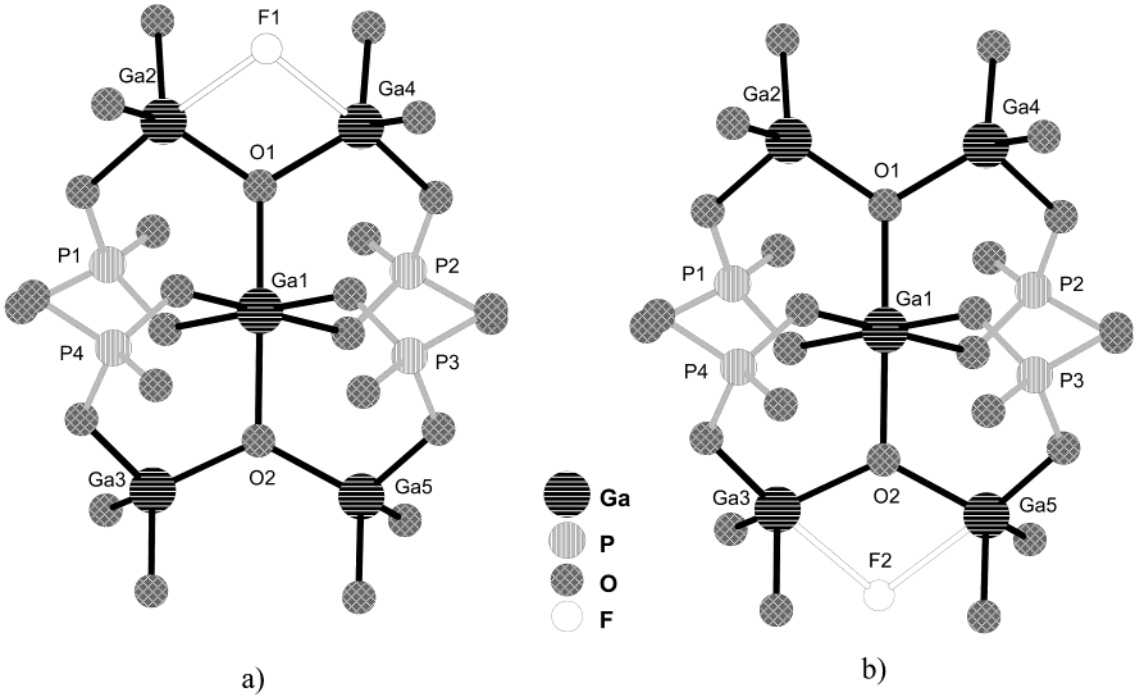

Figure 4. Pentameric building unit of the structure of Mu-12 (based on the number of gallium polyhedra). (a) F(1) bridging Ga(2) and Ga(4) atoms (78% of asymmetric units) and (b) F(2) bridging Ga(3) and Ga(5) atoms (22% of the asymmetric units).

large electron cloud which extended predominantly in the [100] direction. The best result of the refinement was obtained when the N(2) site was split into three positions (N(21), N(22), and N(23)) with identical isotropic displacement parameters. We interpret this result as follows: the N(21) position (occupancy factor = 0.28) is taken if the F(2) position is in fact occupied by fluorine, leading to N(21)−F(2) distances of 2.759 Å (see Figure 7). When the F(2) position is free of fluorine, the N(2) atom moves closer to the oxygen atoms of the framework with contacts: d(N(22)−O(4)) = 2.895 Å, d(N(22)−O(17)) = 2.866 Å, d(N(23)−O(4)) = 2.785 Å, and d(N(23)−O(16)) = 2.866 Å (see Figure 7).

The different positions of the N(2) atom can be achieved by a rotation about the C−C bond. This rotation has only a small effect on the positions of C(1), C(2), and N(1). Split positions could not be refined for these three atoms but relatively high values of the displacement parameters indicate a slight positional variation of C(1), C(2), and N(1). It is likely that the $-N(1)H_3$ group, which is bonded to the F(1) site (78% occupancy by fluorine), also takes another position if the F(1) site is not occupied (22% of the asymmetric units). These other possible positions, however, could not be resolved by the structure refinement.

3.5. ^{13}C NMR Spectroscopy. The ^{13}C CP MAS NMR spectrum of the pure Mu-12 sample (sample B, Table 1) reported in Figure 8 displays two peaks at 39.5 and 40.4 ppm (reference TMS), corresponding to the two carbons of the CH_2 groups. The presence of these two signals is in perfect agreement with the structure determination that shows the existence of two distinct

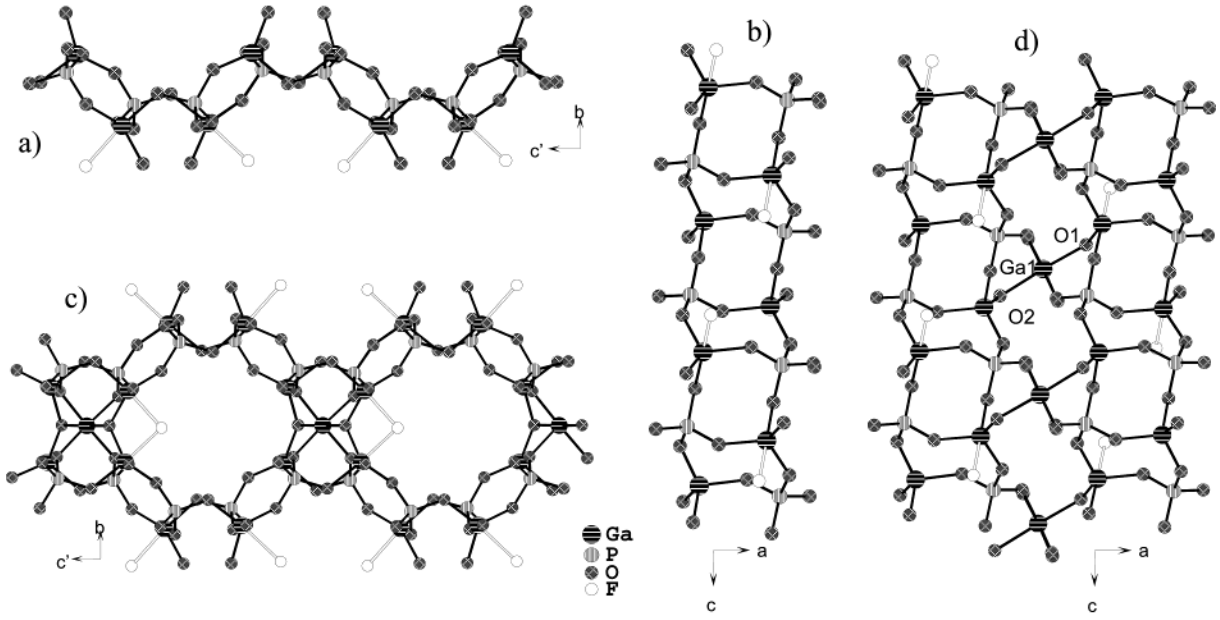

Figure 5. Ladder chain built from single-four rings [Ga_2P_2] viewed along the [100] (a) and [010] (b) directions. Connection of two adjacent chains with the pentameric unit in *b* (c) and *a* (d) directions. (For clarity, the organic template is omitted and only the F(1) position is shown) ($c' = c \sin \beta$).

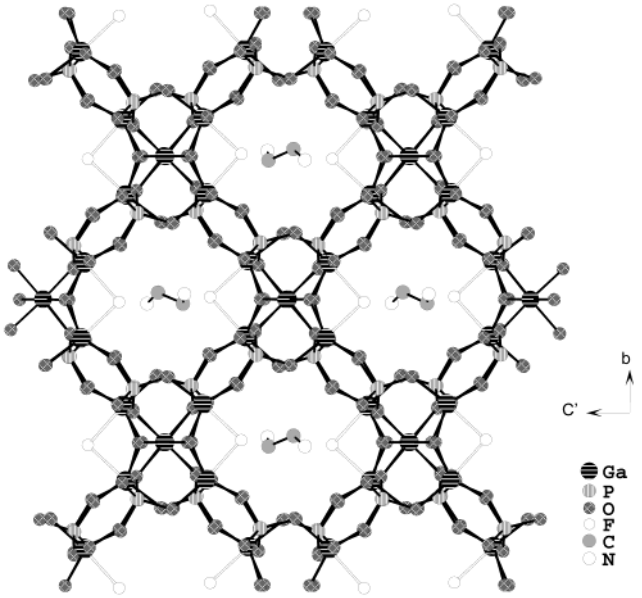

Figure 6. Projection of the structure of Mu-12 along the [100] direction showing the one-dimensional channel system delimited by 9-MR openings and the location of the organic template. (For clarity, only the N(21) position is shown among the three split positions N(21), N(22), and N(23)) ($c' = c \sin \beta$).

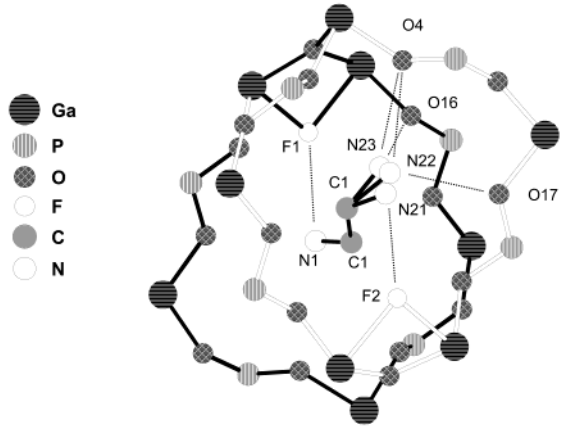

Figure 7. Positions of the carbon and nitrogen atoms of the ethylenediammonium cation in the 9-MR channel showing the splitting of the N(2) position (see text). The N(21) position is taken when the F(2) position is occupied by fluorine and the N(22) and N(23) positions are taken when the F(1) position is occupied by fluorine.

crystallographic sites for the carbon atoms of the ethylenediammonium cation.

3.6. ^{19}F NMR Spectroscopy. The ^{19}F MAS NMR spectrum of the title compound is given in Figure 9. Although the structure refinement shows that the fluorine atom is distributed over two crystallographic positions, only one resonance is observed at −82.3 ppm (reference $CFCl_3$). On the basis of the structure, it corresponds to the bridging fluorine atom (Ga−F−Ga). However, the chemical shift value is quite unusual. For fluorogallophosphates presenting such an environment for F atoms, a signal at around −100 to −110 ppm is expected, as is the case for the fluorogallophosphates Mu-17[29] and $GaPO_4$−CHA.[30] This low-field chemical shift might be due to the large Ga−F bond length. The latter equal to 0.22 (F(1)) or 0.23 nm (F(2)) is relatively close to that observed for a fluorine atom trapped inside a double four-ring unit ($d_{Ga-F} = 0.24$ nm), which leads to a NMR signal at −70 ppm.

3.7. ^{31}P NMR Spectroscopy. The ^{31}P MAS and CP MAS NMR spectra of Mu-12 are very similar. As an example, the ^{1}H-decoupled ^{31}P MAS NMR spectrum, given in Figure 10, displays four different signals with the following chemical shifts: −5.3, −6.5, −9.4, and −10.9 ppm (reference 85% H_3PO_4). The intensity ratio is close to 1:1:1:1. These four signals correspond to the four distinct crystallographic phosphorus sites. For

(29) Matijasic, A.; Gramlich, V.; Patarin, J. *Solid State Sci.* **2001**, *3*, 155.
(30) Schott-Darie, C.; Kessler, H.; Soulard, M.; Gramlich V.; Benazzi, E. *Studies in Surface Science and Catalysis*; Weitkamp, J., Karge, H. K., Pfeifer, H., Hölderich, W., Eds.; Elsevier: Amsterdam, 1994; Vol. 84a, p 101.

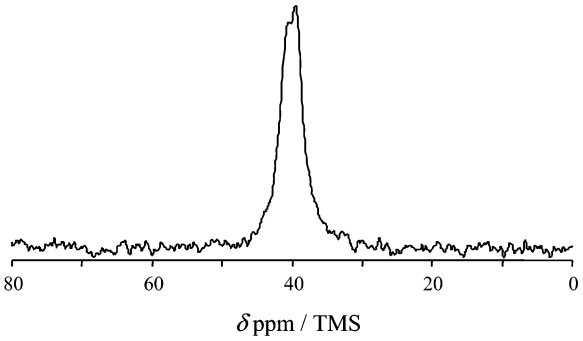

Figure 8. ^{13}C CP MAS NMR spectrum of the fluorogallophosphate Mu-12.

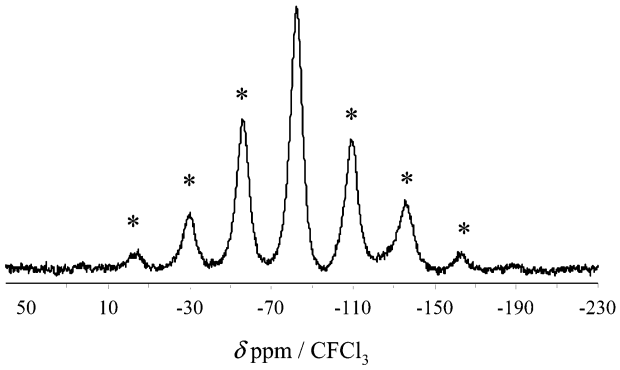

Figure 9. ^{19}F MAS NMR spectrum of the fluorogallophosphate Mu-12 (*: spinning sidebands).

microporous gallophosphates, chemical shift values ranging from −10 to −20 ppm correspond generally to Q^4 groups ($P(OGa)_4$), whereas values close to −5 ppm are usually assigned to Q^3 groups ($HO-P(OGa)_3$). However, in Mu-12 there are no Q^3 groups since all the phosphorus atoms are connected to gallium atoms via oxygens. Moreover, whatever the contact time, no significant differences are observed between the MAS and CP MAS spectra, which indicates, in agreement with the structure determination, that no terminal P−OH groups are present. The small component at −8.5 ppm with no intensity relationships with the other signals corresponds probably to traces of impurity.

4. Conclusion

The use of 4,9-dimethyl-5,8-diaza-dodeca-2,4,8,10-tetraen-2,11-diol (3DTD) or ethylenediamine, in a fluoride-containing gallophosphate mixture, led to the synthesis of a new microporous material, named Mu-12. However, the in situ formation of ethylenediamine by thermal decomposition of 3DTD seems to be the key point for obtaining the title compound as pure phase. Indeed, the direct introduction of ethylenediamine into the starting gel leads systematically to the formation of a mixture of Mu-12 and the fluorogallophosphate ULM-4.

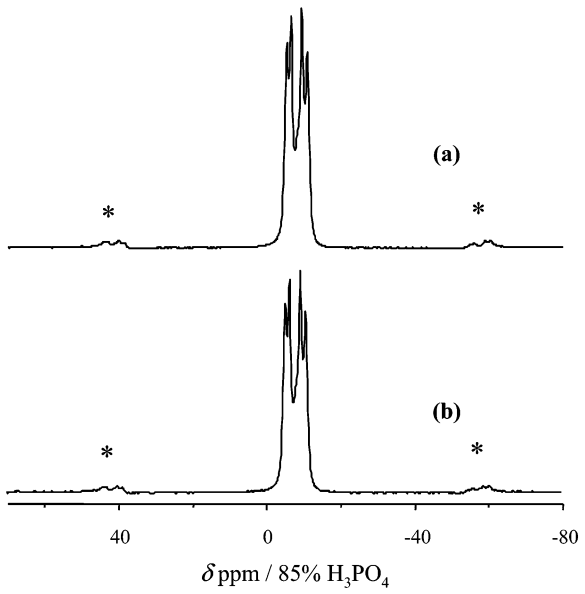

Figure 10. ^{31}P NMR spectra of the fluorogallophosphate Mu-12: (a) MAS spectrum; (b) $^1H-^{31}P$ CP MAS spectrum (*: spinning sidebands).

The three-dimensional structure of Mu-12 solved from single-crystal X-ray data displays a one-dimensional channel system with nine-membered ring openings occluding the ethylenediammonium cations. One interesting feature of this new structure is the presence of GaO_6 octahedra, GaO_4F pentahedra, and GaO_4 polyhedra, which constitutes a new example of the ability of gallium atom to adopt various coordinations and lead to new structures.

As often observed for numerous gallophosphates, it is difficult to open the porosity of this new compound since the complete removal of the organics leads to a collapse of the structure.

Acknowledgment. The authors would like to thank "Institut Français du Pétrole" (IFP), which kindly provided the gallium nitrate source. J.C.M.A. is a grateful recipient of a DAAD scholarship.

Supporting Information Available: A crystallographic CIF file of Mu-12. This material is available free of charge via the Internet at http://pubs.acs.org.

CM021370K